



Effect of Radiation on Transient Natural Convection Flow between Two Vertical Walls

C. Mandal

Department of Mathematics
Vidyasagar University
Midnapore 721 102, India

S. Das

Department of Mathematics
University of Gour Banga
Malda 732 103, India

R. N. Jana

Department of Applied Mathematics
Vidyasagar University
Midnapore 721 102, India

ABSTRACT

The effects of radiation on transient natural convection of a viscous incompressible fluid confined between vertical walls have been studied. We have considered the two different cases (i) flow due to the impulsive motion and (ii) flow due to accelerated motion of one of the walls. The governing equations are solved analytically using the Laplace transform technique. The variations of velocity and fluid temperature are presented graphically. It is observed that the velocity increases for both the impulsive motion as well as the accelerated motion of one of the walls with an increase in radiation parameter. It is also observed that the velocity decreases with an increase in either Prandtl number or time for both the impulsive motion as well as the accelerated motion. An increase in Grashof number leads to a fall in velocity due to enhancement in buoyancy force. An increase in the radiation parameter leads to increase the temperature of the flow field. Further, the shear stress at the moving wall increases for both the impulsive motion as well as the accelerated motion of one of the walls with an increase in radiation parameter. The rate of heat transfer increases with an increase in either radiation parameter or Prandtl number while it decreases with an increase in time.

Keywords

Transient natural convection, radiation, Prandtl number, Grashof number, impulsive motion and accelerated motion

1. INTRODUCTION

In space technology applications and at higher operating temperatures, radiation effects can be quite significant. Since radiation is quite complicated, many aspects of its effect on free convection or combined convection have not been studied in recent years. Radiative convective flows are frequently encountered in many scientific and environmental processes such as astrophysical flows, water evaporation from open reservoirs, heating and cooling of chambers and solar power technology. Heat transfer by simultaneous radiation and convection has applications in numerous technological problems including combustion, furnace design, the design of high temperature gas cooled nuclear reactors, nuclear reactor safety, fluidized bed heat exchanger, fire spreads, solar fans, solar collectors, natural convection in cavities, turbid water bodies, photo chemical reactors and many others. Joshi [1] has studied the transient effects in natural convection cooling of vertical parallel plates. Singh [2] has studied the effect of free convection in unsteady Couette motion between two vertical parallel plates. The transient free convection flow between two vertical parallel plates has been investigated by Singh et al. [3]. Jha et al. [4] have studied the transient free convection flow in a vertical channel due to symmetric heating. A transient study of coupled natural convection and radiation in a porous vertical channel have been

studied by Slimi et al. [5]. Singh and Paul [6] have described the transient natural convection between two vertical walls heated/cooled asymmetrically. The combined radiative and convective heat transfer in a divided channel have been investigated by Bouali and Mezrhab [7]. Thermal radiation effect on fully developed mixed convection flow in a vertical channel has been studied by Grosan and Pop [8]. Rao [9] has analyzed the interaction of surface radiation with conduction and convection from a vertical channel with multiple discrete heat sources in the left wall. The natural convection in unsteady Couette flow between two vertical parallel plates in the presence of constant heat flux and radiation has been presented by Narahari [10]. Attia [11] has discussed the effect of variable properties on the unsteady Couette flow with heat transfer considering the Hall effect. Al-Amri et al. [12] have studied the combined forced convection and surface radiation between two parallel plates. Narahari [13] has investigated the effects of thermal radiation and free convection currents on the unsteady Couette flow between two vertical parallel plates with constant heat flux at one boundary. The radiation effects on free convection MHD Couette flow started exponentially with variable wall temperature in presence of heat generation have been studied by Das et al. [14].

The object of the present investigation is to study the effects of radiation on transient natural convection of a viscous incompressible fluid confined between two infinite vertical walls. It is observed that the velocity u_1 increases for both impulsive motion as well as for accelerated motion of one of the walls with an increase in radiation parameter. It is also observed that the velocity decreases with an increase in either Prandtl number Pr or time τ for both impulsive motion as well as for accelerated motion. An increase in Grashof number Gr leads to a fall in the values of velocity due to enhancement in buoyancy force. An increase in the radiation parameter R leads to an increase in the temperature. Further, it is seen that the shear stress τ_x at the moving wall increases for both impulsive motion as well as for accelerated motion of one of the walls with an increase in radiation parameter R . The rate of heat transfer $-\theta'(0)$ at the wall $\eta = 0$ increases with an increase in either radiation parameter R or Prandtl number Pr while it decreases with an increase in time τ .

2. FORMULATION OF THE PROBLEM AND ITS SOLUTIONS

Consider the unsteady natural convective flow of a viscous incompressible radiating fluid between two infinite vertical parallel walls separated by a distance h . Choose a cartesian

co-ordinates system with the x - axis along one of the walls in the vertically upward direction and the y - axis normal to the walls [See Fig.1]. Initially, at time $t \leq 0$, the two walls and the fluid are assumed to be at the same temperature T_h and stationary. At time $t > 0$, the wall at $y = 0$ starts moving in its own plane with a velocity $U(t)$ and is heated with temperature T_0 whereas the wall at $y = h$ is stationary and maintained at a constant temperature T_h . It is also assumed that the radiative heat flux in the x - direction is negligible as compared to that in the y - direction. As the walls are infinitely long, the velocity and temperature fields are functions of y and t only.

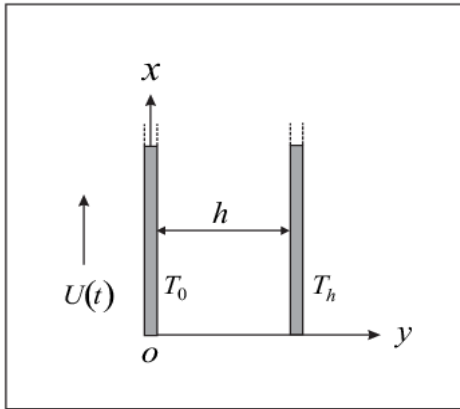


Fig 1 : Geometry of the problem

The Boussinesq approximation is assumed to hold and for the evaluation of the gravitational body force, the density is assumed to depend on the temperature according to the equation of state

$$\rho = \rho_0 [1 - \beta(T - T_h)], \quad (1)$$

where T is the fluid temperature, ρ the fluid density, β the coefficient of thermal expansion and ρ_0 the temperature at the entrance of the channel.

Then under the usual Boussinesq's approximation, the flow of a radiating fluid is shown to be governed by the following system of equations:

$$\frac{\partial u}{\partial t} = -\frac{1}{\rho} \frac{\partial p}{\partial x} + g\beta(T - T_h) + \nu \frac{\partial^2 u}{\partial y^2}, \quad (2)$$

$$\rho c_p \frac{\partial T}{\partial t} = k \frac{\partial^2 T}{\partial y^2} - \frac{\partial q_r}{\partial y}, \quad (3)$$

where u is the fluid velocity in the x -direction, g the acceleration due to gravity, ν the kinematic coefficient of viscosity, ρ the fluid density, k the thermal conductivity, c_p the specific heat at constant pressure and q_r the radiative heat flux.

The initial and the boundary conditions for velocity and temperature distributions are

$$\begin{aligned} u = 0, T = T_h \text{ for } 0 \leq y \leq h \text{ and } t \leq 0, \\ u = U(t), T = T_0 \text{ at } y = 0 \text{ for } t > 0, \\ u = 0, T = T_h \text{ at } y = h \text{ for } t > 0. \end{aligned} \quad (4)$$

It has been shown by Cogley et al.[15] that in the optically thin limit for a non-gray gas near equilibrium, the following relation holds

$$\frac{\partial q_r}{\partial y} = 4(T - T_h) \int_0^\infty K_{\lambda h} \left(\frac{\partial e_{\lambda h}}{\partial T} \right) d\lambda, \quad (5)$$

where $K_{\lambda h}$ is the absorption coefficient, λ is the wave length, $e_{\lambda h}$ is the Planck's function and subscript 'h' indicates that all quantities have been evaluated at the temperature T_h which is the temperature of the wall at time $t \leq 0$. Thus our study is limited to small difference of wall temperature to the fluid temperature.

On the use of the equation (5), equation (3) becomes

$$\rho c_p \frac{\partial T}{\partial t} = k \frac{\partial^2 T}{\partial y^2} - 4(T - T_h)I, \quad (6)$$

where

$$I = \int_0^\infty K_{\lambda h} \left(\frac{\partial e_{\lambda h}}{\partial T} \right) d\lambda. \quad (7)$$

We introduce non-dimensionless variables

$$\eta = \frac{y}{h}, \tau = \frac{\nu t}{h^2}, u_1 = \frac{u}{U_0}, \theta = \frac{T - T_h}{T_0 - T_h}, U(t) = U_0 f(\tau). \quad (8)$$

On the use of (8), equations (2) and (6) become

$$\frac{\partial u_1}{\partial \tau} = \frac{\partial^2 u_1}{\partial \eta^2} + Gr\theta + P, \quad (9)$$

$$Pr \frac{\partial \theta}{\partial \tau} = \frac{\partial^2 \theta}{\partial \eta^2} - R\theta, \quad (10)$$

where $R = \frac{4Ih^2}{k}$ the radiation parameter,

$Gr = \frac{g\beta(T_0 - T_h)h^2}{\nu U_0}$ the Grashof number, $Pr = \frac{\rho \nu c_p}{k}$ the

Prandtl number and $P = -\frac{h^2}{\rho \nu h_0} \frac{\partial p}{\partial x}$ the non-dimensional pressure.

The corresponding initial and boundary conditions for u_1 and θ are

$$\begin{aligned} u_1 = 0, \theta = 0 \text{ for } 0 \leq \eta \leq 1 \text{ and } \tau \leq 0, \\ u_1 = f(\tau), \theta = 1 \text{ at } \eta = 0 \text{ for } \tau > 0, \\ u_1 = 0, \theta = 0 \text{ at } \eta = 1 \text{ for } \tau > 0. \end{aligned} \quad (11)$$

Taking Laplace transformation of the equations (9) and (10), we get

$$s\bar{u}_1 = \frac{d^2 \bar{u}_1}{d\eta^2} + Gr\bar{\theta} + \frac{P}{s}, \quad (12)$$

$$Prs\bar{\theta} = \frac{d^2 \bar{\theta}}{d\eta^2} - R\bar{\theta}, \quad (13)$$

where

$$\bar{u}_1(\eta, s) = \int_0^\infty u_1(\eta, \tau) e^{-s\tau} d\tau \text{ and } \bar{\theta}(\eta, s) = \int_0^\infty \theta(\eta, \tau) e^{-s\tau} d\tau. \quad (14)$$

The corresponding boundary conditions for \bar{u}_1 and $\bar{\theta}$ are

$$\begin{aligned} \bar{u}_1(0, s) = f(s), \bar{\theta}(0, s) = \frac{1}{s}, \\ \bar{u}_1(1, s) = 0, \bar{\theta}(1, s) = 0, \end{aligned} \quad (15)$$

where $f(s)$ is the Laplace transform of the function $f(t)$.

The solution of the equations (13) and (12) subject to the boundary conditions (15) are easily obtained and are given by



$$\bar{\theta}(\eta, s) = \frac{1}{s} \frac{\sinh \lambda(1-\eta)}{\sinh \lambda} \quad \text{where } \lambda = \sqrt{R + sPr}, \quad (16)$$

$$\begin{aligned} \bar{u}_1(\eta, s) = f(s) & \frac{\sinh \sqrt{s}(1-\eta)}{\sinh \sqrt{s}} \\ & + \frac{P}{s^2} \left[1 - \frac{\sinh \sqrt{s}\eta}{\sinh \sqrt{s}} - \frac{\sinh \sqrt{s}(1-\eta)}{\sinh \sqrt{s}} \right] \\ & + \frac{Gr}{s[R + (Pr-1)s]} \\ & \times \left[\frac{\sinh \sqrt{s}(1-\eta)}{\sinh \sqrt{s}} - \frac{\sinh \sqrt{R+sPr}(1-\eta)}{\sinh \sqrt{R+sPr}} \right]. \quad (17) \end{aligned}$$

Now, we shall consider the following cases:

(i) **When one of the plate ($\eta = 0$) started impulsively:**

In this case $f(\tau) = 1$, i.e. $f(s) = \frac{1}{s}$. Then the inverse

transforms of equations (16) and (17) give the solution for the temperature and the velocity distributions as

$$\theta(\eta, \tau) = \frac{\sinh \sqrt{R}(1-\eta)}{\sinh \sqrt{R}} - 2\pi \sum_{n=1}^{\infty} n(-1)^n \frac{e^{s_1 \tau}}{Pr s_1} \sin n\pi\eta, \quad (18)$$

$$\begin{aligned} u_1(\eta, \tau) = (1-\eta) & + \frac{1}{2} P\eta(1-\eta) + \frac{Gr}{R} \left[(1-\eta) - \frac{\sinh \sqrt{R}(1-\eta)}{\sinh \sqrt{R}} \right] \\ & + 2\pi \sum_{n=1}^{\infty} n \left[\frac{e^{s_2 \tau}}{s_2} \left\{ 1 + \frac{(-1)^n P}{s_2} - \frac{P}{s_2} \right\} \right. \\ & \left. + Gr \left\{ \frac{e^{s_2 \tau}}{s_2[R + (Pr-1)s_2]} - \frac{e^{s_1 \tau}}{Pr s_1[R + (Pr-1)s_1]} \right\} \right] \sin n\pi\eta, \quad (19) \end{aligned}$$

where

$$s_1 = -\frac{n^2 \pi^2 + R}{Pr}, \quad s_2 = -n^2 \pi^2 \quad (20)$$

and the value of the pressure P is evaluated from the condition

$$\int_0^1 u_1 d\eta = 1. \quad (21)$$

In the steady state ($\tau \rightarrow \infty$), equations (18) and (19) become

$$\theta(\eta) = \frac{\sinh \sqrt{R}(1-\eta)}{\sinh \sqrt{R}} \quad (22)$$

$$\begin{aligned} u_1(\eta) = (1-\eta) & + \frac{1}{2} P\eta(1-\eta) \\ & + \frac{Gr}{R} \left[(1-\eta) - \frac{\sinh \sqrt{R}(1-\eta)}{\sinh \sqrt{R}} \right] \quad (23) \end{aligned}$$

(ii) **When one of the plate ($\eta = 0$) started accelerately:**

In this case $f(\tau) = \tau$, i.e. $f(s) = \frac{1}{s^2}$. Then the inverse

transforms of equations (16) and (17) yield

$$\theta(\eta, \tau) = \frac{\sinh \sqrt{R}(1-\eta)}{\sinh \sqrt{R}} - 2\pi \sum_{n=1}^{\infty} n(-1)^n \frac{e^{s_1 \tau}}{Pr s_1} \sin n\pi\eta, \quad (24)$$

$$u_1(\eta, \tau) = \tau(1-\eta) + \frac{1}{6} \eta(1-\eta)(\eta-2)$$

$$\begin{aligned} & + \frac{1}{2} P\eta(1-\eta) + \frac{Gr}{R} \left[(1-\eta) - \frac{\sinh \sqrt{R}(1-\eta)}{\sinh \sqrt{R}} \right] \\ & + 2\pi \sum_{n=1}^{\infty} n \left[\frac{e^{s_2 \tau}}{s_2^2} \left\{ 1 + (-1)^n P - P \right\} \right. \\ & \left. + Gr \left\{ \frac{e^{s_2 \tau}}{s_2[R + (Pr-1)s_2]} - \frac{e^{s_1 \tau}}{Pr s_1[R + (Pr-1)s_1]} \right\} \right] \sin n\pi\eta, \quad (25) \end{aligned}$$

where s_1 and s_2 are given by (20) and the pressure P is evaluated from the condition (21).

In the steady state ($\tau \rightarrow \infty$), the values of the temperature and the velocity distributions are given by

$$\theta(\eta) = \frac{\sinh \sqrt{R}(1-\eta)}{\sinh \sqrt{R}}, \quad (26)$$

$$\begin{aligned} u_1(\eta) = \tau(1-\eta) & + \frac{1}{6} \eta(1-\eta)(\eta-2) + \frac{1}{2} P\eta(1-\eta) \\ & + \frac{Gr}{R} \left[(1-\eta) - \frac{\sinh \sqrt{R}(1-\eta)}{\sinh \sqrt{R}} \right]. \quad (27) \end{aligned}$$

3. EVALUATION OF PRESSURE

On the use of the equation (19), equation (21) gives the pressure P of the fluid due to impulsive motion of the wall at ($\eta = 0$) as

$$\begin{aligned} P = & \left[\frac{1}{2} - \frac{Gr}{R} \left(\frac{1}{2} + \frac{1 - \cosh \sqrt{R}}{\sqrt{R} \sinh \sqrt{R}} \right) \right. \\ & \left. - 2 \sum_{n=1}^{\infty} \left\{ (-1)^n - 1 \right\} \left[\frac{e^{s_2 \tau}}{s_2} + Gr \left\{ \frac{e^{s_2 \tau}}{s_2[R + (Pr-1)s_2]} \right. \right. \right. \\ & \left. \left. \left. - \frac{e^{s_1 \tau}}{Pr s_1[R + (Pr-1)s_1]} \right\} \right] \right] / \left[\frac{1}{12} + 2 \sum_{n=1}^{\infty} \left\{ (-1)^n - 1 \right\}^2 \frac{e^{s_2 \tau}}{s_2^2} \right]. \quad (28) \end{aligned}$$

In the steady state motion, we have

$$P = 12 \left[\frac{1}{2} - \frac{Gr}{R} \left(\frac{1}{2} + \frac{1 - \cosh \sqrt{R}}{\sqrt{R} \sinh \sqrt{R}} \right) \right]. \quad (29)$$

Similarly, for the accelerated start of the wall at ($\eta = 0$), the fluid pressure P is obtained by using equation (25) in the equation (21) as

$$\begin{aligned} P = & \left[1 - \frac{\tau}{2} - \frac{Gr}{R} \left(\frac{1}{2} + \frac{1 - \cosh \sqrt{R}}{\sqrt{R} \sinh \sqrt{R}} \right) \right. \\ & \left. - \frac{e^{s_1 \tau}}{Pr s_1[R + (Pr-1)s_1]} \right] / \left[\frac{1}{12} + 2 \sum_{n=1}^{\infty} \left\{ (-1)^n - 1 \right\}^2 \frac{e^{s_2 \tau}}{s_2^2} \right] \quad (30) \end{aligned}$$

and for steady state motion, we get

$$P = 12 \left[1 - \frac{\tau}{2} - \frac{Gr}{R} \left(\frac{1}{2} + \frac{1 - \cosh \sqrt{R}}{\sqrt{R} \sinh \sqrt{R}} \right) \right]. \quad (31)$$

3. RESULTS AND DISCUSSION

We have presented the non-dimensional velocity and temperature distributions for several values of radiation parameter R , Prandtl number Pr , Grashof number Gr and time τ in Figs.2-8 after evaluation of P from equations (28) and (30) for both the impulsive motion as well as the accelerated motion of one of the walls. Figs.2-5 represent the velocity u_1 against η for several values of R , Pr , Gr and τ . It is seen



from Fig.2 that the velocity u_1 increases for both impulsive motion and accelerated motion of one of the wall with an increase in radiation parameter R . Fig.3 shows that the velocity u_1 decreases for both impulsive motion as well as for accelerated motion with an increase in Prandtl number Pr . Physically, this is true because the increase in the Prandtl number is due to increase in the viscosity of the fluid which makes the fluid thick and hence causes a decrease in the velocity of the fluid. It is observed from Fig.4 that an increase in Gr leads to fall in the values of velocity u_1 due to enhancement in buoyancy force. It is seen from Fig.5 that the velocity u_1 decreases for both impulsive motion and accelerated motion of one of the wall with an increase in time τ . Figs.2-5 show that the velocity in case of accelerated start of one of the wall is larger than that of the impulsive start. It is seen from Fig.6 that the temperature θ decreases as the radiation parameter R increases. This result qualitatively agrees with expectations, since the effect of radiation is to decrease the rate of energy transport to the fluid, thereby decreasing the temperature of the fluid. It is observed from Fig.7 that the temperature θ decreases with an increase in Prandtl number Pr . This implies that an increase in Prandtl number leads to fall the thermal boundary layer flow. The effect of the Prandtl number is very important in the temperature field. A fall in temperature occurs due to an increasing value of the Prandtl number. This is in agreement with the physical fact that the thermal boundary layer thickness decreases with increasing Pr . Fig.8 reveals that the temperature θ increases with an increase in time τ which implies that there is an enhancement in fluid temperature as time progresses.

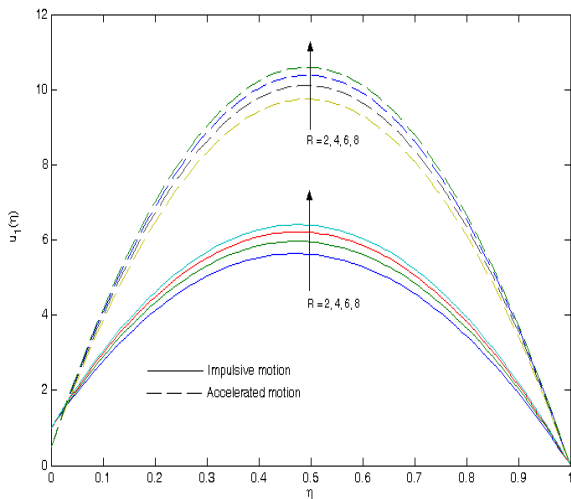


Fig 2: Velocity profiles for R when $Pr = 0.71$, $Gr = 5$ and $\tau = 0.5$

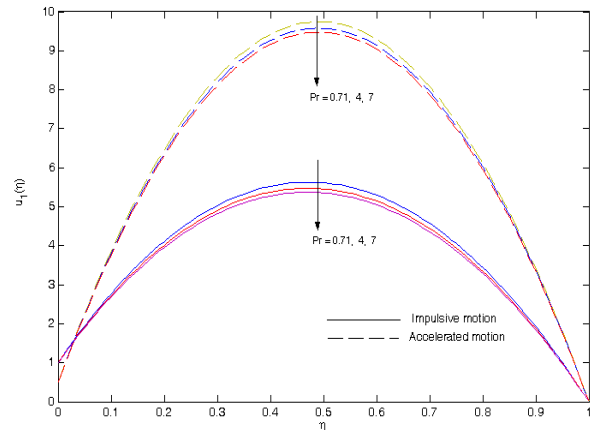


Fig 3: Velocity profiles for Pr when $R = 2$, $Gr = 5$ and $\tau = 0.5$

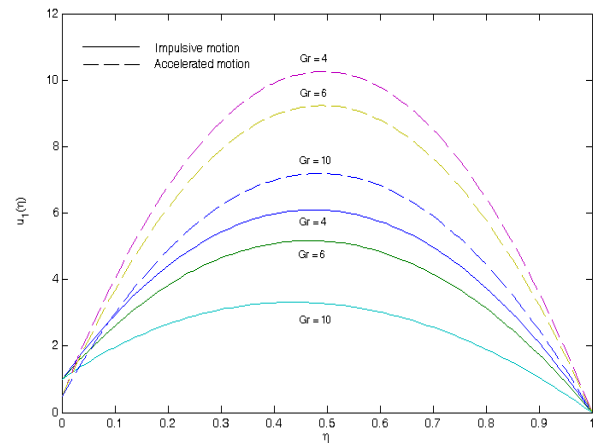


Fig4: Velocity profiles Gr when $Pr = 0.71$, $R = 2$ and $\tau = 0.5$

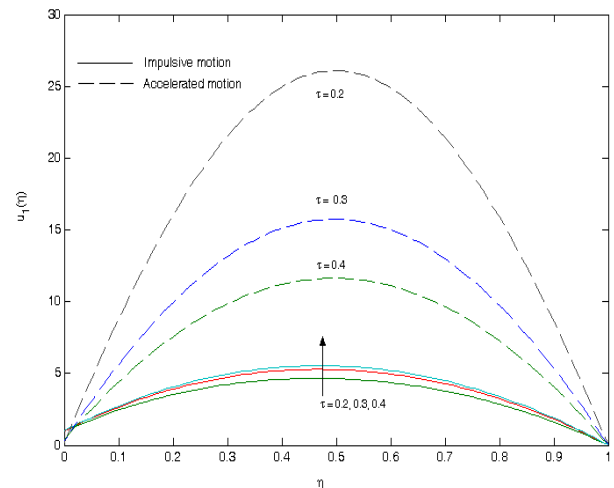


Fig 5: Velocity profiles for β when $Pr = 0.71$, $R = 2$ and $Gr = 5$

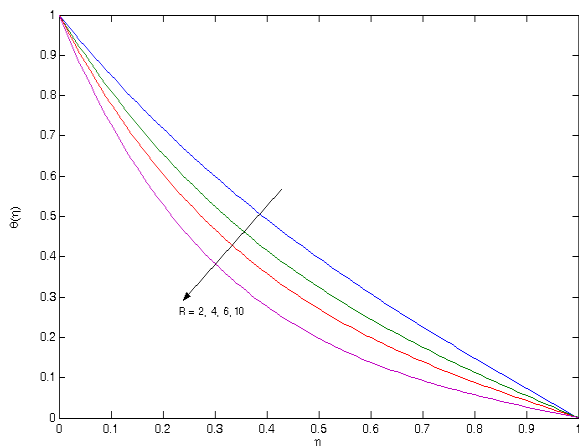


Fig 6: Temperature profiles for R when $Pr = 0.71$ and $\tau = 0.5$

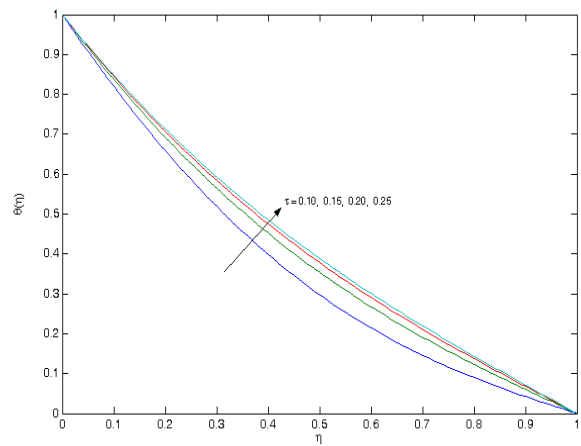


Fig 8: Temperature profiles for time τ when $Pr = 0.71$ and $R = 2$

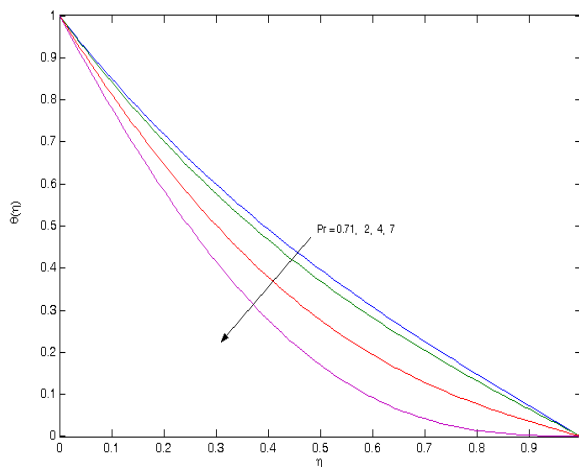


Fig.7: Temperature profiles for Pr when $R = 2, \beta = 1$ and $\tau = 0.2$

Numerical values of fluid pressure P calculated from equations (28) and (30) due to the flow are presented in Tables 1-3 for several values of radiation parameter R , Prandtl number Pr , Grashof number Gr and time τ . Table 1 shows that for both impulsive as well as the accelerated start of one of the walls, the fluid pressure P increases with an increase in R while it decreases with an increase in Gr for fixed values of Pr and time τ . It is observed from Table 2 that for both impulsive as well as accelerated start of one of the walls, the fluid pressure P decreases with an increase in Pr for fixed values of Gr and τ . Further, Table 3 shows that the fluid pressure P increases with an increase in time τ for both the impulsive as well as the accelerated start of the wall at $\eta = 0$.

Table 1. Variation of pressure P when $Pr = 0.71$ and $\tau = 0.5$

$R \backslash Gr$	Impulsive Motion				Accelerated motion			
	4	6	8	10	4	6	8	10
2	0.43407	0.35029	0.26651	0.18273	0.73545	0.65167	0.56788	0.48410
4	0.45792	0.38606	0.31420	0.24234	0.75929	0.68743	0.61557	0.54371
6	0.47575	0.41281	0.34986	0.28692	0.77712	0.71418	0.65124	0.58830
8	0.48959	0.43357	0.37755	0.32153	0.79097	0.73495	0.67893	0.62291

Table 2. Variation of pressure P when $Gr = 5$ and $\tau = 0.5$

$R \backslash Pr$	Impulsive Motion				Accelerated motion			
	0.71	2	4	5	0.71	2	4	5
2	0.39218	0.39012	0.38597	0.38437	0.69356	0.69149	0.68735	0.68575
4	0.42199	0.42070	0.41755	0.41621	0.72336	0.72208	0.71892	0.71759
6	0.44428	0.44345	0.44103	0.43992	0.74565	0.74483	0.74241	0.74130
8	0.46158	0.46103	0.45917	0.45824	0.76296	0.76241	0.76054	0.75961



Table 3. Variation of pressure P when $Pr = 0.71$ and $Gr = 5$

$R \setminus \tau$	Impulsive Motion				Accelerated motion			
	0.1	0.2	0.3	0.4	0.1	0.2	0.3	0.4
2.0	0.35967	0.37723	0.38655	0.39058	0.90187	0.85990	0.80883	0.75237
4.0	0.39037	0.40779	0.41672	0.42050	0.93258	0.89046	0.83900	0.78229
6.0	0.41330	0.43055	0.43922	0.44286	0.95550	0.91322	0.86150	0.80465
8.0	0.43106	0.44817	0.45666	0.46020	0.97327	0.93084	0.87894	0.82199

The rate of heat transfer at the wall $\eta = 0$ is obtained as

$$-\theta'(0) = -\frac{\partial \theta}{\partial \eta} \Big|_{\eta=0} = \sqrt{R} \coth \sqrt{R} + 2\pi^2 \sum_{n=1}^{\infty} n^2 \frac{e^{-s_1 \tau}}{s_1}, \quad (32)$$

where s_1 is given by (20).

Numerical results of the rate of heat transfer at the wall $\eta = 0$ against the radiation parameter R are presented in the Figs.9-10 for various values of Prandtl number Pr and time τ . Fig.9 shows that the rate of heat transfer $-\theta'(0)$ increases with an increase in either radiation parameter R or Prandtl number Pr . It is observed from Fig.10 that for fixed value of R , the rate of heat transfer $-\theta'(0)$ decreases with an increase in timer τ .

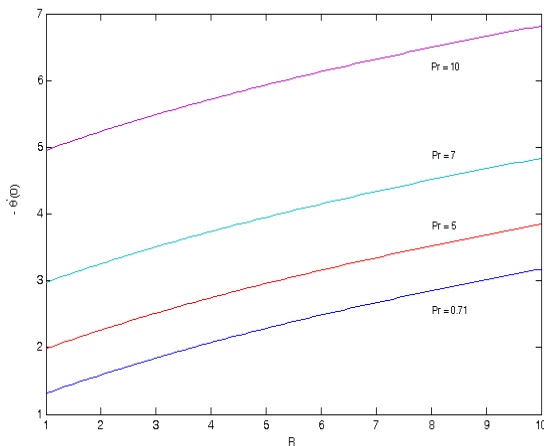


Fig 9: Rate of heat transfer $-\theta'(0)$ for Pr when $\tau = 0.5$

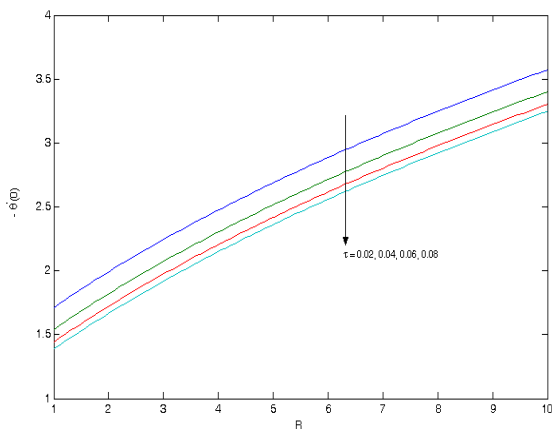


Fig 10: Rate of heat transfer $-\theta'(0)$ for time τ when $Pr = 0.71$

For impulsive motion, the non-dimensional shear stress at the

plate $\eta = 0$ is give by

$$\tau_x = \frac{\partial u_1}{\partial \eta} \Big|_{\eta=0} = -1 + \frac{1}{2}P - \frac{Gr}{R} (1 - \sqrt{R} \coth \sqrt{R}) + 2\pi^2 \sum_{n=1}^{\infty} n^2 \left[\frac{e^{-s_2 \tau}}{s_2} \left\{ 1 + \frac{(-1)^n P}{s_2} - \frac{P}{s_2} \right\} + Gr \left\{ \frac{e^{-s_2 \tau}}{s_2 [R + (Pr-1)s_2]} - \frac{e^{-s_1 \tau}}{Pr s_1 [R + (Pr-1)s_1]} \right\} \right]. \quad (33)$$

For steady state, τ_x is given by

$$\tau_x = -1 + \frac{1}{2}P - \frac{Gr}{R} [1 - \sqrt{R} \coth \sqrt{R}]. \quad (34)$$

For accelerated motion, the non-dimensional shear stress at the plate $\eta = 0$ is obtained as

$$\tau_x = \frac{\partial u_1}{\partial \eta} \Big|_{\eta=0} = -\tau - \frac{1}{3} + \frac{1}{2}P - \frac{Gr}{R} (1 - \sqrt{R} \coth \sqrt{R}) + 2\pi^2 \sum_{n=1}^{\infty} n^2 \left[\frac{e^{-s_2 \tau}}{s_2^2} \{ 1 + (-1)^n P - P \} + Gr \left\{ \frac{e^{-s_2 \tau}}{s_2 [R + (Pr-1)s_2]} - \frac{e^{-s_1 \tau}}{Pr s_1 [R + (Pr-1)s_1]} \right\} \right], \quad (35)$$

where s_1 and s_2 are given by (20).

For steady state, τ_x is given by

$$\tau_x = -\tau - \frac{1}{3} + \frac{1}{2}P - \frac{Gr}{R} [1 - \sqrt{R} \coth \sqrt{R}]. \quad (36)$$

Numerical results of the non-dimensional shear stress at the wall ($\eta = 0$) are presented in Figs.11-13 against Grashof number Gr for various values of radiation parameter R , Prandtl number Pr and time τ . Fig.11 shows that the shear stress τ_x increases for both impulsive as well as accelerated start of one of the walls with an increase in either Grashof number Gr or radiation parameter R . Fig.12 displays that the shear stress τ_x decreases with an increase in Prandtl number Pr for both the cases of impulsive and accelerated motions of one of the walls. It is observed from Fig.13 that for both the impulsive as well as the accelerated start of one of the walls the shear stress τ_x decreases with an increase in time τ . Further, it is observed from Figs.11-13 that the shear stress τ_x at the plate ($\eta = 0$) for the accelerated start of one of the wall is greater than that of the impulsive start. These results are in agreement with the fact that the velocity increases with an increase in Gr while it decreases with an increases in either Pr or τ .

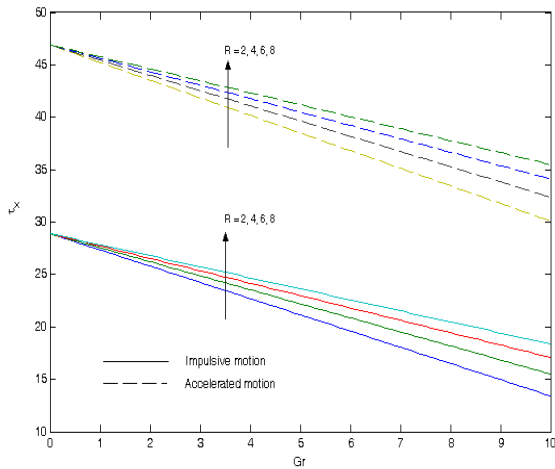


Fig 11: Shear stress τ_x for R when $Pr = 0.71$ and $\tau = 0.5$

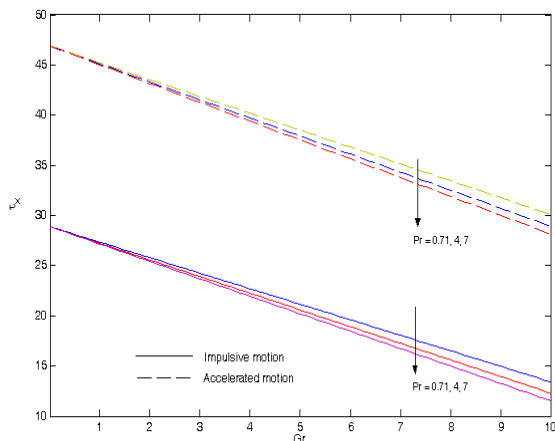


Fig 12: Shear stress τ_x for Pr when $R = 2$ and $\tau = 0.5$

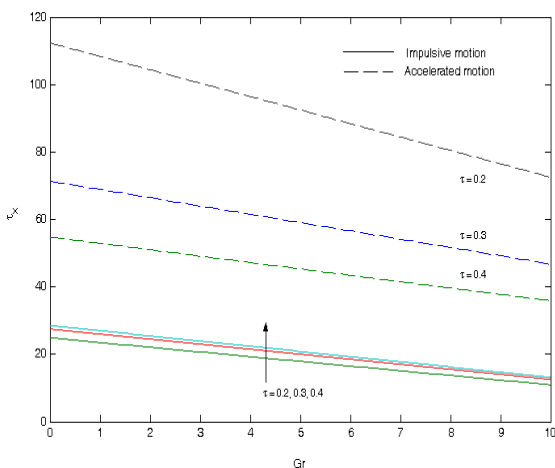


Fig 13: Shear stress τ_x for time τ when $Pr = 0.71$ and $R = 2$

5. CONCLUSION

The radiation effects on transient natural convection flow confined between two infinitely long vertical walls have been

studied. It is observed that for both the impulsive motion as well as for the accelerated motion of one of the walls the fluid velocity u_1 increases with an increase in radiation parameter. It is also observed that the fluid velocity u_1 decreases with an increase in either Prandtl number Pr or time τ for both the impulsive motion as well as for the accelerated motion. An increase in Grashof number Gr leads to a fall in the fluid velocity u_1 due to enhancement in buoyancy force. An increase in the radiation parameter R leads to rise in the fluid temperature. The effect of the Prandtl number is very important in the temperature field. Further, the shear stress τ_x at the moving wall at $\eta = 0$ increases for both the impulsive motion as well as for the accelerated motion with an increase in radiation parameter R . The rate of heat transfer $-\theta'(0)$ at the wall at $\eta = 0$ increases with an increase in either radiation parameter R or Prandtl number Pr while it decreases with an increase in time τ .

6. REFERENCES

- [1] Joshi, H. M. 1988. Transient effects in natural convection cooling of vertical parallel plates. *Int. Comm. Heat Mass Transfer*. 15, 227-238.
- [2] Singh, A. K. 1988. Natural convection in unsteady Couette motion. *Defense Science Journal*, 38(1), 35-41.
- [3] Singh, A. K., Gholami, H. R. and Soundalgekar, V. M. 1996. Transient free convection flow between two vertical parallel plates. *Heat and Mass Transfer*. 31, 329-331.
- [4] Jha, B. K., Singh, A. K. and Takhar, H. S. 2003. Transient free convection flow in a vertical channel due to symmetric heating. *Int. J. Appl. Mech. Eng.* 8(3), 497-502.
- [5] Slimi, K., Zili-Ghedira, L., Ben Nasrallah, S. and Mohamad, A. A. 2004. A transient study of coupled natural convection and radiation in a porous vertical channel using the finite-volume method. *Numer. Heat Transfer Part A*. 45, 451-478.
- [6] Singh, A. K. and Paul, T. 2006. Transient natural convection between two vertical walls heated/cooled asymmetrically. *Int. J. Appl. Mech. Eng.* 11(1), 143-154.
- [7] Bouali, H. and Mezrhab, A. 2006. Combined radiative and convective heat transfer in a divided channel. *Int. J. Num. Meth. Heat Fluid Flow*. 16, 84-106.
- [8] Grosan, T. and Pop, I. 2007. Thermal radiation effect on fully develop mixed convection flow in a vertical channel. *Technische Mechanik*, 27(1), 37-47.
- [9] Rao, C.G. 2007. Interaction of surface radiation with conduction and convection from a vertical channel with multiple discrete heat sources in the left wall. *Numer. Heat Transfer Part A : Appl.* 52, 831-848.
- [10] Narahari, M. Natural convection in unsteady Couette flow between two vertical parallel plates in the presence of constant heat flux and radiation. *MACMESE'09 Proceedings of the 11th WSEAS international conference on Mathematical and computational methods in science and engineering*.
- [11] Al-Amri, Fahad G., El-Shaarawi, Maged A.I. 2010. Combined forced convection and surface radiation between two parallel plates. *Int. J. Numerical Methods for Heat &*



Fluid Flow. 20(2), 218-239 .

- [12] Narahari, M. 2010. Effects of thermal radiation and free convection currents on the unsteady couette flow between two vertical parallel plates with constant heat flux at one boundary. WSEAS Transactions on Heat and Mass Transfer, 5(1), 21-30.
- [13] Das, S., Sarkar, B. C. and Jana, R. N. 2012. Radiation effects on free convection MHD Couette flow started exponentially with variable wall temperature in presence of heat generation. Open J. Fluid Dynamics, 2, 14-27.
- [14] Cogley, A.C., Vincentine, W.C. and Gilles, S.E. 1968. A Differential approximation for radiative transfer in a non-gray gas near equilibrium. AIAA Journal. 6, 551-555.